Mn^{4+} cation localization in La-rich La$_{1-x}$Ca$_x$MnO$_y$ manganites

J. Alonso,[1] E. Herrero,[1] J. M. González-Calbet,[1] M. Vallet-Regí,[1] J. L. Martinez,[2] J. M. Rojo,[3] and A. Hernando[1]

[1]*Instituto de Magnetismo Aplicado, UCM, CSIC, RENFE, Las Rozas, P.O. Box 155, Madrid 28230, Spain*
[2]*ICMM, CSIC, Cantoblanco, 28049 Madrid, Spain*
[3]*Departamento de Física de Materiales, UCM, 28040 Madrid, Spain*

Magnetization and electrical resistivity have been measured in La$_{1-x}$Ca$_x$MnO$_y$ manganites in the ranges $0.00 \leq x \leq 0.25$ and $2.90 \leq y \leq 3$. The magnetization is found to depend primarily on the concentration of Mn^{4+}. A small concentration of substitutional Ca ions ($x \approx 0.50-0.10$) is found to suppress the onset of metallic behavior even for Mn^{4+} concentrations of 0.25. A model is proposed that assumes localization of Mn^{4+} cations around Ca substitutional atoms resulting in ferromagnetic clusters that are locally conducting. Percolation of these clusters, attained after increasing the Ca concentration to $x \approx 0.25$, leads to long-range metallic behavior. We propose that Mn^{4+} localization is due to differences in local Jahn-Teller splitting that is higher near the La sites than near the Ca ones.

The magnetic phase diagram and the transport properties of $Ln_{1-x}D_x$MnO$_3$ (Ln: lanthanide, D: divalent ion) perovskites, particularly in the region where ferromagnetic (FM) and antiferromagnetic (AFM) ordering coexist, is still a matter of controversy.[1–4] Much of the current research effort has been triggered by the urge to understand the peculiar behavior of the electrical conductivity of these materials, particularly the origin of the so-called colossal magnetoresistance and the characteristics of a metal-insulator transition in the close neighborhood of the Curie temperature T_C. This T_C characterizes the transition from a low-temperature FM to a high-temperature paramagnetic (PM) state. Experiments using different techniques, from neutron scattering and nuclear magnetic resonance (NMR) to magnetization measurements,[5,6] describe the FM state in terms of either a canted AFM structure or a two-phase state formed by segregated regions of FM and AFM ordering. Concerning the mechanisms underlying the FM ordering and the onset of metallic conduction, it has been realized that the double exchange mechanism, proposed by Zener[7] and extended by de Gennes,[8] requires to be complemented by the inclusion of lattice distortion effects,[9,10] leading to a rather complex theoretical phase diagram as a function of the doping concentration x and temperature T. Nevertheless, some predictions, such as the existence of FM polaronic clusters[2] involving three Mn, seem to be confirmed by recent experiments.[4] The latter also propose that following an increasing x, these FM clusters first grow and finally attain the metallic state by percolation.

In the La$_{1-x}$Ca$_x$MnO$_y$ perovskite structure, Mn^{4+} holes can be generated either by *substitution* of divalent Ca for La ions in the center of the cubes or by *oxidation* of the initially vacancy-rich LaMnO$_3$ but in previous investigations it was currently assumed that only the *total* concentration of Mn^{4+} was of relevance. As a consequence of this assumption, the role of substitutional ions (Ca^{2+}) was restricted to that of supplying Mn^{4+} to the system. In this paper, we report experiments starting at x as low as 0.05, in which the magnetic and resistive properties of La$_{1-x}$Ca$_x$MnO$_y$ samples with similar concentration of Mn^{4+} but very different concentration of substitutional ions are compared. This is done by carefully controlling the concentration of anionic and cationic vacancies. Our results are at variance with the above assumption and, in fact, show that whereas the partial fraction of Mn^{4+} holes indeed governs the degree of FM order, this is not the case in regard to the appearance of a metallic state. An interesting phenomenon is disclosed at low Ca concentrations (down to $x = 0.05$): the presence of a low concentration of Ca ions actually hinders the onset of a metallic state even for Mn^{4+} concentrations higher than $x = 0.25$. We propose that in the presence of Ca, the metallic state cannot be attained because percolation is thwarted as a result of the generation around the Ca ions of clusters consisting of cation vacancies and Mn^{4+} sites. To explain this behavior, a simple model is proposed in terms of a different Jahn-Teller splitting depending on the Mn localization in the neighborhood of either La or Ca ions.

Air synthesized powder La$_{1-x}$Ca$_x$MnO$_y$ materials (A_x samples) were prepared by solid-state reaction of stoichiometric amounts of La$_2$O$_3$, CaCO$_3$, and MnO$_2$ with repeated grindings and firings at temperatures up to 1400 °C for 110 h and finally quenched down to room temperature. Oxidized compounds (O_x samples) were obtained by annealing A_x samples at 1300 °C for 24 h under an oxygen flow. These materials were cooled (rate$=2$ K min^{-1}) to room temperature inside the furnace under oxygen flow. The chemical composition of all the samples is shown in Table I following a complete control of cationic composition, oxygen content, and oxidation state of Mn atoms. Note that the cationic and anionic vacancy contents of every batch of samples are indicated by the corresponding subindex. We believe this vacancy control to be mandatory as discrepancies among phase diagrams from different authors are likely to arise from inadequate control of the sample compositions. Cationic ratios were determined by inductive coupling plasma. Oxygen content and therefore the Mn^{4+}/Mn^{3+} ratio was determined by thermogravimetric analysis in a CAHN-D200 electrobalance. Magnetic susceptibilities were measured with a superconducting quantum interference device (SQUID) magnetometer and electrical resistance measurements carried out by the four contacts method using a physical properties measuring system (PPMS, Quantum Design). All samples exhibited the perovskite-type structure with orthorhombic symmetry

TABLE I. Chemical composition and unit cell parameters of $La_{1-x}Ca_xMnO_y$ perovskites.

Sample	Composition	Unit-cell parameters		
		a (nm)	b (nm)	c (nm)
$A_{0.00}$[a]	$La_{0.96}(Mn^{4+}_{0.18}Mn^{3+}_{0.82})_{0.96}O_{2.97(1)}$	0.5572(2)	0.5572(2)	1.339(3)
$A_{0.05}$	$(La_{0.95}Ca_{0.05})_{0.96}(Mn^{4+}_{0.09}Mn^{3+}_{0.91})_{0.96}O_{2.90(1)}$	0.5600(2)	0.5519(2)	0.7715(3)
$A_{0.10}$	$(La_{0.90}Ca_{0.10})_{0.97}(Mn^{4+}_{0.14}Mn^{3+}_{0.86})_{0.97}O_{2.93(1)}$	0.5577(2)	0.5515(1)	0.7748(3)
$A_{0.20}$	$(La_{0.80}Ca_{0.20})_{0.99}(Mn^{4+}_{0.24}Mn^{3+}_{0.76})_{0.99}O_{2.99(1)}$	0.5487(1)	0.5488(1)	0.7766(3)
$A_{0.25}$	$(La_{0.75}Ca_{0.25})(Mn^{4+}_{0.25}Mn^{3+}_{0.75})O_{2.99(1)}$	0.5472(1)	0.5473(1)	0.7766(3)
$O_{0.00}$[a]	$La_{0.96}(Mn^{4+}_{0.25}Mn^{3+}_{0.75})_{0.96}O_{3.00(1)}$	0.5536(3)	0.5536(3)	1.337(2)
$O_{0.05}$[a]	$(La_{0.95}Ca_{0.05})_{0.96}(Mn^{4+}_{0.29}Mn^{3+}_{0.71})_{0.96}O_{3.00(1)}$	0.5512(2)	0.5512(2)	1.336(3)
$O_{0.10}$	$(La_{0.90}Ca_{0.10})_{0.97}(Mn^{4+}_{0.28}Mn^{3+}_{0.72})_{0.97}O_{3.00(1)}$	0.5501(3)	0.5495(3)	0.7745(3)
$O_{0.20}$	$(La_{0.80}Ca_{0.20})_{0.99}(Mn^{4+}_{0.27}Mn^{3+}_{0.73})_{0.99}O_{3.00(1)}$	0.5483(2)	0.5476(2)	0.7738(3)
$O_{0.25}$	$(La_{0.75}Ca_{0.25})(Mn^{4+}_{0.27}Mn^{3+}_{0.73})O_{3.00(1)}$	0.5458(2)	0.5454(2)	0.7734(3)

[a]Rhombohedral symmetry. Parameters correspond to the hexagonal cell.

(space group Pnma) except the $O_{0.05}$ material which showed rhombohedral symmetry (space group $R\bar{3}c$). Unit-cell parameters are gathered in Table I. Electron-diffraction patterns did not show superstructure spots suggesting that anionic vacancies are randomly distributed. Were there some order present, it would be nonperiodic and would contribute only to the incoherent background between Bragg reflections in the diffraction pattern.

Figure 1 shows the thermal dependence of magnetization and electrical resistance for the rich-in-oxygen-vacancies samples $A_{0.05}$ and $A_{0.25}$, whereas Fig. 2 does the same for

fully oxidized samples $O_{0.05}$ and $O_{0.25}$. We remark on the following characteristics: (i) Magnetic properties: The results of Figs. 1(a) and 2(a) indicate that, at 1000 Oe applied field, the low-temperature magnetization is practically the same for samples $A_{0.25}$ and $O_{0.25}$ and similar (within $\sim$10%) for $O_{0.05}$, in all cases being close to 50 emu g^{-1}. Notice that the saturation magnetization requires an external field about five times higher as shown in the inset of Fig. 1(a). The percentages of Mn^{4+}, relative to the total Mn content, are also similar for the three samples—respectively, 25, 27 and 27%—but the Ca cations concentration is different, 25% for samples
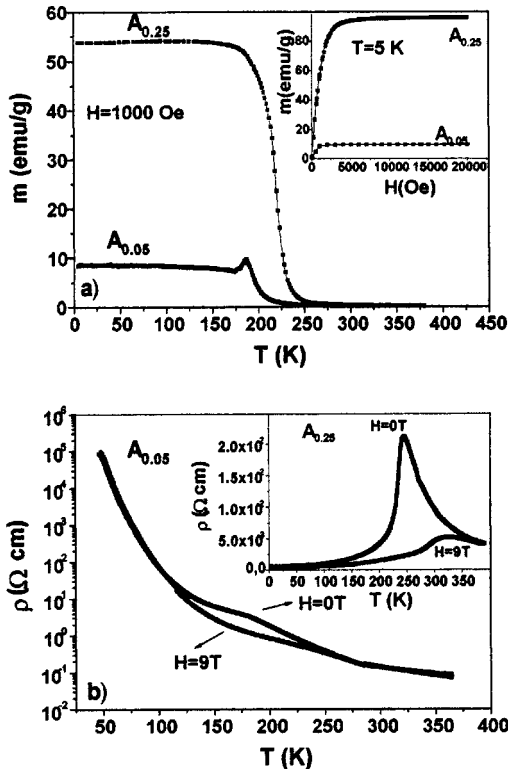

FIG. 1. (a) Thermal dependence of magnetization, measured under 1000 Oe applied field, for samples $A_{0.05}$ and $A_{0.25}$. Inset: Saturation curve for the $A_{0.05}$ and $A_{0.25}$ samples. (b) Electrical resistance dependence on T for the same samples.
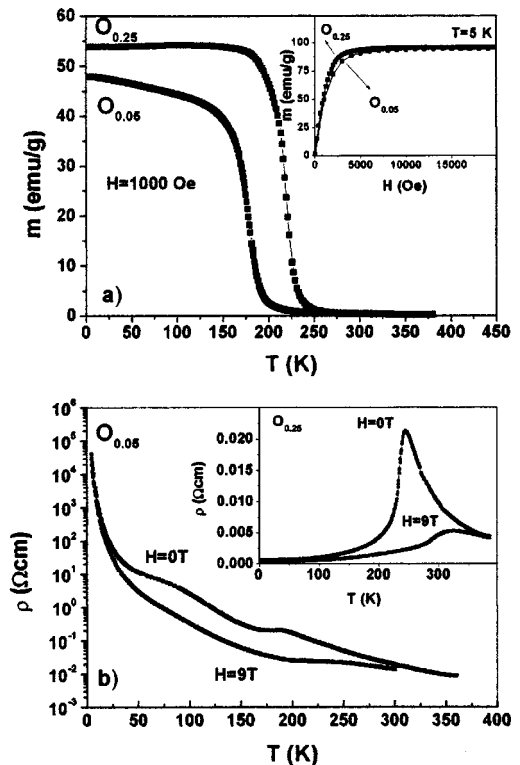
FIG. 2. (a) Thermal dependence of magnetization, measured under 1000 Oe applied field, for samples $O_{0.05}$ and $O_{0.25}$. Inset: Saturation curve for the $O_{0.05}$ and $O_{0.25}$ samples. (b) Electrical resistance dependence on T for the same samples.

$A_{0.25}$ and $O_{0.25}$ but only 5% for sample $O_{0.05}$. On the other hand, the sample $A_{0.05}$, with a low content (9%) of Mn^{4+}, has a magnetization of only 9 emu g^{-1}. Notice than upon oxidation of the latter ($A_{0.05} \rightarrow O_{0.05}$), the low-field magnetization increases from 9 emu g^{-1} up to 48 emu g^{-1}. Furthermore, Figs. 1(a) and 2(a) show that the Curie temperature, being equal for $A_{0.25}$ and $O_{0.25}$ decreases about 50 K for $O_{0.05}$. In the weakly ferromagnetic sample $A_{0.05}$ the effective Curie temperature resembles also that of $O_{0.05}$. (ii) Electrical conduction: As shown in Figs. 1(b) and 2(b), sample $A_{0.05}$ is an insulator in all the temperature range, as expected on the basis of its low Mn^{4+} concentration. Samples $A_{0.25}$ and $O_{0.25}$ are metallic conductors, also in good agreement with other authors' measurements and with expectations based on the concentration of Mn^{4+}, which in both samples attains the 25% percolation theoretical threshold. Note in both samples the large resistance peak near the Curie temperature, which is related to the metallic-insulator transition. However, comparison of their common electrical properties with those of sample $O_{0.05}$ reveals an unexpected behavior. Although all three samples exhibit similar magnetic characteristics, and have also similar Mn^{4+} contents, their behavior vis-à-vis the onset of a metallic state is quite different, the sample $O_{0.05}$ being an insulator in all the range of temperatures. Moreover, the absence of metal-insulator transition is common to samples $A_{0.05}$ and $O_{0.05}$ which contain the same percentage of Ca cations, $\approx 5\%$, despite the threefold increase in the Mn^{4+} fraction introduced by oxidation, which grows from 9% in sample $A_{0.05}$ to 29% in sample $O_{0.05}$. The samples with 10% Ca ($A_{0.10}$ and $O_{0.10}$) behave in much the same way as those with 5% as shown in Fig. 3. On the other hand, when the concentration of Ca is increased into the 20–25% range, the metal-insulator transition appears. In fact the $A_{0.20}$ and $O_{0.20}$ samples have a similar behavior to the $A_{0.25}$ and $O_{0.25}$. (iii) Structural changes: The fivefold increase in magnetization undergone by the $A_{0.05}$ sample during oxidation to $O_{0.05}$ takes place alongside with a structural change from orthorhombic to rhombohedral. In order to have insight into the possible role of the latter, Fig. 3 compares the above process with the effect of oxidation on sample $A_{0.1}$ which evolves towards $O_{0.1}$ *without* any structural change. The relative fraction of Mn^{4+} increases now by oxidation from 14 to 28%. As shown in Fig. 3(a), the low-temperature magnetization, measured under 1000 Oe applied field, increases from 9 emu/g for sample $A_{0.1}$ up to 50 emu/g for sample $O_{0.1}$ indicating a huge effect, in fact, practically the same that the one produced by oxidation of sample $A_{0.05}$. Furthermore, Fig. 3(b) shows that the thermal dependence of the electrical resistance measured for samples $A_{0.1}$ and $O_{0.1}$ is not so strongly affected by oxidation. Both as-prepared and oxidized samples are insulators at all temperatures with only a small feature in the resistive curve around T_C.

These results show that magnetization values, as well as their thermal dependence, are determined primarily by the fraction number of Mn^{4+} holes, independently of the Ca concentration. On the other hand, the resistance data suggest that transport is determined not only by the concentration of Mn^{4+} but by the Ca cations concentration; when this fraction is in the range 5–10% the sample is an insulator independently of a high concentration of doped holes Mn^{4+} (at least, up to the limit of 27%). The Ca concentration needs to be
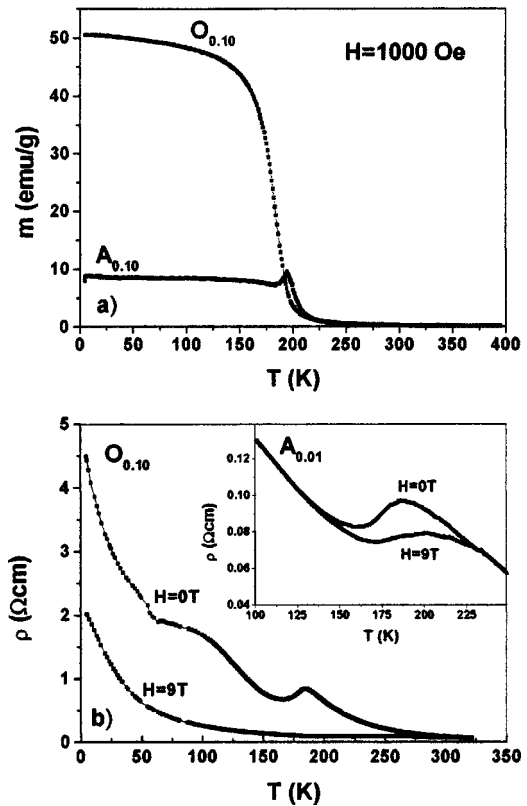

FIG. 3. (a) Thermal dependence of magnetization, under 1000 Oe applied field, for samples $A_{0.10}$ and $O_{0.10}$. Notice the increase of magnetization induced by oxidation of sample $A_{0.10}$. (b) Electrical resistance dependence on T for the same samples.

raised to the range 20–25% to achieve a metal-insulator transition. Indeed, our experiments show that, at low concentrations, Ca substitutional ions do seem to play a role more complex than described hitherto.

Additional insight is gained from further comparison of the magnetic and conductive behavior of samples $A_{0.25}$ and $O_{0.05}$. Low-field magnetization of sample $A_{0.25}$ (25% of Mn^{4+}) is about 11% larger than that of the $O_{0.05}$ sample with practically the same concentration of Mn^{4+}(29%). This suggests an upper limit of about 11% for the volume fraction of sample $O_{0.05}$ which is not ferromagnetic. Surprisingly enough, this 11% of nonferromagnetic volume results in an increase of resistivity of several orders of magnitude with respect to the resistivity of sample $A_{0.25}$, which according to Fig. 1 is ferromagnetic and metallic. This striking difference is directly related to a different Ca content and might be understood by assuming that the introduction of Ca destroys the random character of the Mn^{4+} holes distribution. One might argue that the impossibility of attaining a conductor state is due to a mechanism involving only the cationic vacancies. This possibility can be dismissed by the results of transport measurements, Fig. 4, performed in two undoped $La_{1-x}Mn_{1-x}O_y$ materials: $A_{0.00}$ and $O_{0.00}$ synthesized under the same conditions than the rest of the A and O series. Their chemical composition and x-ray-diffraction data are also listed in Table I. It is worth recalling that both $A_{0.00}$ and $O_{0.00}$ show a similar cationic-vacancy concentration, *higher* than that of sample $O_{0.05}$. This higher concentration of cationic vacancies does not prevent the onset of the metallic state as
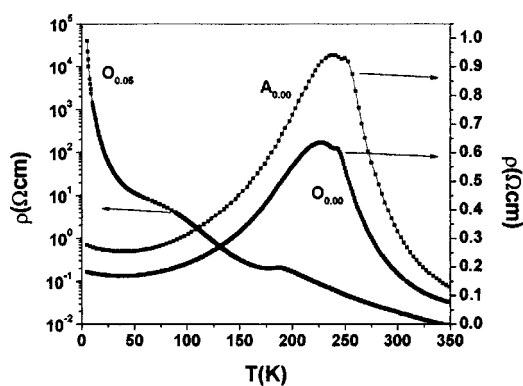
FIG. 4. Electrical resistance dependence on T for the $A_{0.00}$, $O_{0.00}$, and $O_{0.05}$ samples.

shown by the remarkable decrease of the resistance upon applying a field of 9 T in both samples, is in agreement with results in Ca-free samples of other authors.[3,11–16] Comparing these results with the behavior of our sample $O_{0.05}$ (with smaller percentage of Mn vacancies), it is difficult to escape from the conclusion that the lack of a metallic-insullator transition in $O_{0.05}$ is due to the presence of the 5% of Ca cations. It is important to remark that, following oxidation, the orthorhombic LaMnO$_3$ evolves into a rhombohedral structure[14] and that this change of structure is also observed in our sample $O_{0.05}$.

We propose that Mn^{4+} holes are localized around Ca cations forming ferromagnetic clusters. This ferromagnetism would then account for the high value of the magnetization of Fig. 2(a). Carrier confinement into locally conducting clusters with local ferromagnetic ordering has been observed above the ferromagnetic transition temperature T_C in La$_{0.67}$Ca$_{0.33}$MnO$_3$.[17] In that compound the onset of a low-resistive state is reached when cooling down through T_C and interpreted in terms of magnetic polaron breaking. It is then likely that the undistorted clusters around the Ca ions, whose existence we propose, are also locally conducting although the spatial localization imposed by the Ca dopants results in clusters that are electrically isolated from each other. For low x, independently of the Mn^{4+} relative fraction, these clusters only percolate when the Ca cation fraction reaches a concentration near to 25%. The size of the conducting and ferro-

magnetic cluster located around Ca cations can be estimated from the percolation threshold concentration. If we assume the Mn^{4+} cations are located at the corners of cubes centered in Ca cations, percolation should occur when similar cubes are distributed along [111] directions shearing only one corner where a Mn^{4+} cation is placed. This corresponds to a 25% of Ca cations content in fair agreement with experimental observations.

Why are Mn^{4+} holes localized around Ca cations? It is known that in the stoichiometric LaMnO$_3$ the doubly degenerated e_g level at Mn^{3+} sites is splitted by the Jahn-Teller (JT) effect resulting in a full lower band. We tentatively suggest that the JT splitting of a Mn^{3+} located at the neighborhood of Ca ions is smaller than that of Mn^{3+} located around La ions and therefore the energy of creation of a hole (Mn^{3+}→Mn^{4+}) is lower in the neighborhood of a Ca ion. This proposal is founded in the well-known[1,4] decrease of lattice distortion of the La$_{1-x}$D$_x$MnO$_3$ perovskite as x increases from 0 up to 0.33, the latter being the content for which the distortion disappears. Recent work by Louca et al.[18] suggests that for this type of perovskites, doped holes would be repelled by the Mn sites with high JT distortion. It is also worth reminding that CaMnO$_3$ is a very stable compound in which each Ca ion is surrounded by all Mn^{4+} ions. In the clusters that we are regarding, cation vacancies (of Mn and La) in neighboring cubes might play the alternative role of neighbor Ca ions in the stoichiometric CaMnO$_3$ and help thus to stabilize a high concentration of Mn^{4+} around the Ca ions.

In conclusion, we have shown that for $x<0.2$ substitution of Ca for La ions in La$_{1-x}$Ca$_x$MnO$_3$ perovskites does not only lead to an increase of Mn^{4+} holes (as usually assumed) but to actually hindering the onset of the metallic conduction even when the number of Mn^{4+} holes reaches 25%. This is most probably due to the formation of Mn^{4+}-rich, nonpercolating FM clusters around the Ca ions, the tendency of Mn^{4+} holes to concentrate around Ca ions being accounted for by a smaller Jahn-Teller splitting of the levels of the Mn ions situated in the less-distorted neighborhood of Ca ions.

[1] B. Dabrowski et al., Phys. Rev. B **60**, 7006 (1999).
[2] J. S. Zhou et al., Phys. Rev. Lett. **79**, 3234 (1997).
[3] R. Mahendiran et al., Phys. Rev. B **53**, 3348 (1996).
[4] D. Papavassiliou et al., Phys. Rev. B **59**, 6390 (1999).
[5] E. O. Wollan and W. C. Koehler, Phys. Rev. **100**, 545 (1955).
[6] P. Schiffer et al., Phys. Rev. Lett. **75**, 3336 (1995).
[7] C. Zener, Phys. Rev. **81**, 440 (1951).
[8] P. G. de Gennes, Phys. Rev. **118**, 141 (1960).
[9] A. J. Millis et al., Phys. Rev. Lett. **74**, 5144 (1995).
[10] H. Röder et al., Phys. Rev. Lett. **76**, 1356 (1996).

[11] C. N. R. Rao and A. K. Cheetham, Science **272**, 369 (1996).
[12] A. Arulraj et al., J. Solid State Chem. **127**, 87 (1996).
[13] A. K. Cheetham et al., J. Solid State Chem. **126**, 337 (1996).
[14] J. Töpfer and J. B. Goodenough, J. Solid State Chem. **130**, 117 (1997).
[15] K. Fröchlich et al., J. Magn. Magn. Mater. **211**, 67 (2000).
[16] I. Maurin et al., J. Magn. Magn. Mater. **211**, 139 (2000).
[17] J. M. De Teresa et al., Nature (London) **386**, 256 (1997).
[18] D. Louca et al., Phys. Rev. B **56**, 8475 (1997).